



Simulation of a torsional capacitive accelerometer and interface electronics using an analog hardware description language

J.M. Gómez-Cama, O. Ruiz, S. Marco, J.M. López-Villegas, J. Samitier

Enginyeria i Materials Electronics, Department de Física Aplicada i Electrònica, Universitat de Barcelona, Av. Diagonal 645-647, 08028-Barcelona, Spain
Email: santi@iris1.fae.ub.es

Abstract

A clear trend in Microsystems technology is towards the integration of mechanical and electronic functions. In many interfacing approaches, the interaction between the electronics and the mechanical parts is fundamental for the correct operation of the devices. Here we present how this interaction can be handled taking advantage of the possibilities of the analog hardware description languages. This modelling and simulation approach is applied to the joint simulation of a torsional capacitive accelerometer and the interfacing electronics.

Notation

α	Rotation angle	b_2	Long side of the support cross-section
ϵ	Dielectric constant	B	Viscous term
ξ	Damping ratio	C_1	Sensing capacitor long arm
ρ	Silicon density	C_s	Sensing capacitor short arm
a	Thickness of the seismic mass	g	Acceleration
b_1	Short side of the support	g_m	OTA's Transconductance
		G	Silicon shear modulus
		h	Gap

I	Inertial moment	V_f	Input voltage to the gain stage of the OTA
i_g	Output current OTA	V_o	Output voltage
i_{max}	Saturation current OTA	V_{ref}	Reference voltage
l	Seismic mass width	x_o	Distance from the support to the electrode
K	Rotational spring constant	x_1	Length shorter arm
M_g	Acceleration moment	x_2	Length longer arm
M_{v1}	Electrostatic moment in the short arm		
M_{v2}	Electrostatic moment in the long arm		

1. Introduction

Capacitive detection is a common sensing scheme in mechanical sensors. Compared to the piezoresistive alternative, it usually offers a higher sensitivity, minor temperature effects and lower power consumption. However, typical capacitance values in integrated sensors are of the order of several picofarads, and the total variation can be even less than 1 pF. Because of these low capacitance values, they are especially sensitive to parasitic capacitances. To prevent their influence, the current trend is the integration, either in monolithic or hybrid form, of interfacing circuits usually based on switched-capacitor techniques.

However, capacitive detection implies a source of non-linearity when electrostatic forces are able to move the capacitor arms. This effect is especially important in micromachined accelerometers. When they consist on a single capacitance, electrostatic force can cause seismic mass movements and, in consequence, capacitance changes without any acceleration present. For accelerometers in a double-differential capacitance configuration, these electrostatic forces are nulled in the central position. Nevertheless, when the seismic mass moves away from this point, the electrostatic forces are no longer cancelled out and in fact they contribute to the movement of the mass. This fact cause non-linearities in the output of the sensor.

Some interfacing schemes take advantage of this electro-mechanical interaction to obtain a conditioned signal output. They are based on the balance between electrostatic and inertial forces (Force balance)[1]. The interfacing electronics acts as a control circuit which keeps the seismic mass at the central position. The control signal can be made proportional to the applied acceleration. This approach presents two clear advantages: first, as the seismic mass do not move the non-linearities commented above disappear and second, the influence of the viscous damping also disappears.

From a signal flow-graph point of view, this kind of interfaces are characterized because part of the signal flow is non-electrical. This introduces the main topic of this work: the design-flow of these systems can no longer be based in standard electronic CAD tools. It is necessary to move towards environments which permit the joint simulation of interacting elements where the signals belong to different physical disciplines.

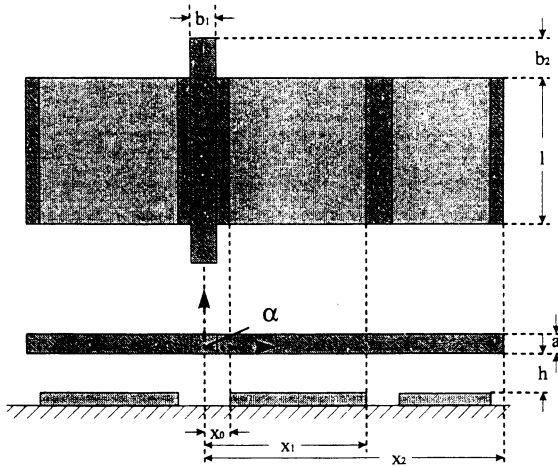


Fig. 1 Scheme of the mechanical structure of the accelerometer.

2. Description of the accelerometer

The sensor to be modeled in this work is a capacitive torsional accelerometer obtained by bulk micromachining[2]. The mechanical structure, that is shown in figure 1, is a plate of uniform thickness ($10\ \mu\text{m}$) suspended by two non-centered bridges. The plate is $3400\ \mu\text{m}$ long and $1400\ \mu\text{m}$ wide. The supports are $200\ \mu\text{m}$ long and $28\ \mu\text{m}$ wide. At both sides of the supports, the plate is the movable arm of a capacitor with the fixed aluminum plates located above in a bonded Pyrex wafer. The accelerometer uses a double-differential capacitance. With the seismic mass at rest, both capacitors are equal valued.

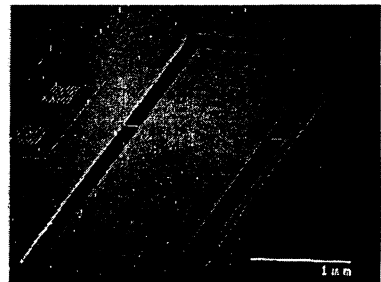
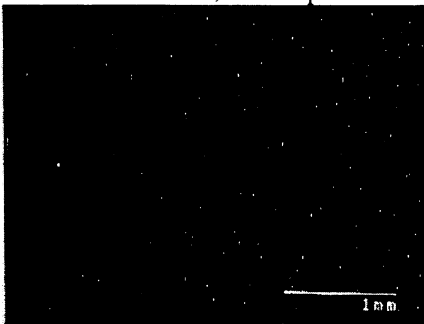


Fig. 3 SEM images of the accelerometers.

However, when an acceleration is present, the mass rotates around the supports causing an unbalance in the capacitances. This unbalance has to be sensed by the interfacing circuitry. In figure 2 and 3 you can see the SEM images of the fabricated microdevices. You may notice the presence of holes in the plate aiming to reduce the very large damping coefficient due to the nearness between the seismic mass and the PYREX substrate (2 μm).

3. Accelerometer model

The following discussion applies to the accelerometer without holes. To model the behaviour of the accelerometer, we consider a system with a single degree of freedom: the rotation angle around the supports. This kind of movement corresponds to the first vibration mode. Finite Element Simulation show that the first natural frequency appears at 1 KHz, and the second mode at 5 KHz.

Despite these values, the accelerometer is overdamped and the cut frequency of the system is just 10 Hz corresponding to a damping ratio of 102. This is due to the absence of holes. Consequently, it is expected that any possible excitation of the second mode would be attenuated. In fact, the experimental measurements show no relevant peak at this frequency, being the accelerometer response attenuated by more than 40 dB.

Hence, the movement of the seismic mass can be represented approximately by a second order system:

$$I \frac{d^2\alpha}{dt^2} + B \frac{d\alpha}{dt} + K\alpha = M_g + M_{v1} + M_{v2} \quad (1)$$

Note, that this equation represents a coupled electro-mechanical problem. With the help of this description we will be able to explore the interactions between the interfacing circuitry and the mechanical structure.

It is necessary now to give values to the parameters and external momentums acting on the structure. The inertial moment can be easily calculated from the geometric dimensions of the seismic mass:

$$I = \frac{1}{3} \rho l a (x_2^3 + x_1^3) \quad (2)$$

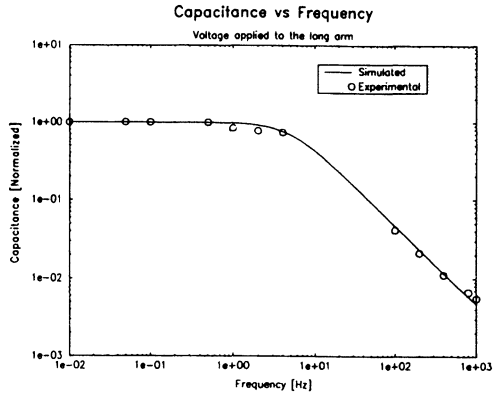


Fig. 4 Fitted small-signal transfer function of the accelerometer. (Damping -B- is the fitting parameter).

We choose to calculate the K from FEM simulations, which permit to include the effects of filets near the extremes of the supports. In the FEM model we apply a moment using force loads at the extremes of the seismic mass. From the resulting torsional angle we deduce the value of K . The calculus of the viscous term is not trivial at all. We relied on the experimental measurement of the transfer function of the accelerometer where B was left as the only fitting parameter. The transfer function can be observed in figure 4.

Lets calculate now, the force moment acting on the structure. On the one hand, the moment due to acceleration:

$$M_g = \frac{1}{2} \rho l a (x_2^2 - x_1^2) g \quad (3)$$

The force moment due to the electrostatic forces is given by:

$$M_v = \frac{e l}{\alpha^2} \left[\frac{\alpha h (x_0 - x_1)}{(h + \alpha x_0)(h + \alpha x_1)} + \ln \left(\frac{h + \alpha x_1}{h + \alpha x_0} \right) \right] V^2 \quad (4)$$

We observe that this moment is quadratic on the applied voltage (as it is the electrostatic force).

Up to now, we have studied the structure from the mechanical point of view. For the joint simulation of the interface circuit we also need its capacitance, which for both capacitors is given by:

$$C = \frac{e l}{\alpha} \ln \left(\frac{h + \alpha x_1}{h + \alpha x_0} \right) \quad (5)$$

Despite the formula above is non-linear, for low values of α it presents a linear behaviour. In fact the expected non-linearity is 3% in the range -5 g to 5 g .

This model predicts the correct static behaviour of the structure against excitations caused by the acceleration and by the applied voltage. Figure 5 shows the variation of the capacitance versus the applied voltage. A quadratic dependence appears, the total capacitance variation is also the expected, but we observe that the minimum of the parabola does not appear centered at zero voltage. This behaviour is due to the presence of a capacitance in series with the mobile electrode. In the positive

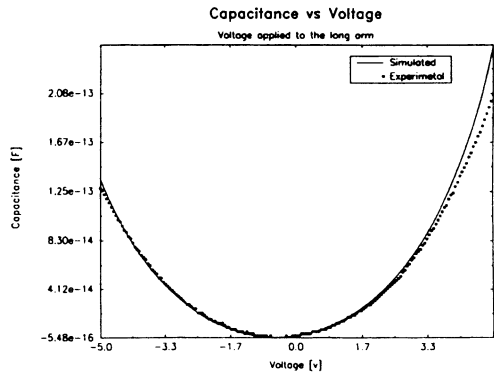


Fig. 5 Capacitance versus voltage.

polarization of the seismic mass a positive charge has to appear in the surface of an n-doped electrode. This implies the formation of a depletion zone and a series capacitor in consequence.

4. Interfacing electronics

Although a number of interfacing schemes can be used to obtain a useful signal from a double-differential capacitive sensor, the more common ones are: (i) Charge-amplifier, (ii) Charge-balance, (iii) Force-balance.

In this work, we will analyze the performance of these schemes by the analysis of the total system described with an Analog Hardware Description Language, namely HDL-A from ANACAD-Mentor Graphics.

In the first scheme, the clock signal causes a change in the polarization state of the sensing capacitors. By balancing the charge between the two clock states a voltage signal appears in the common arm which gives the signal proportional to the acceleration (figure 6)[3]. It is the only configuration without feedback and does nothing to correct the influence of the electrostatic forces. It is the usual configuration in double-differential macroscopic capacitive sensors.

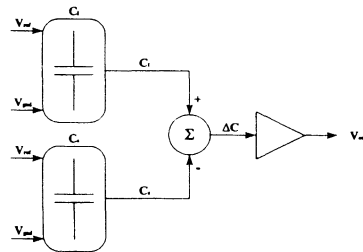


Fig. 6 Functional scheme of a charge amplifier.

In the second interfacing technique, the measuring scheme is designed to create symmetrical forces on the plate. By doing so, it cancels out the non-linearity induced by the electrostatic forces. The name 'charge-balance' comes from the fact that by balancing the electrostatic forces we are also balancing the charges in both capacitors. However, up to now this scheme has been applied only to double-differential plane-parallel capacitors where the seismic mass moves perpendicular to the electrodes. We will analyze its performance for a torsional accelerometer. Let's analyze briefly how this can be achieved by means of the scheme in figure 7. To do that, let's consider

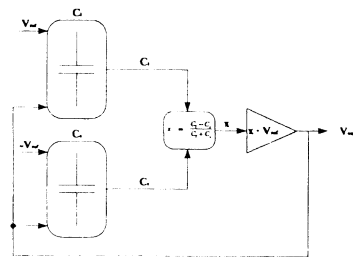


Fig. 7 Functional scheme of a charge-balance.

We will analyze its performance for a torsional accelerometer. Let's analyze briefly how this can be achieved by means of the scheme in figure 7. To do that, let's consider

a parallel accelerometer. The electrostatic forces acting on the seismic mass are:

$$F = \frac{\epsilon A}{2} \left[\frac{(V_{ref} - V_{out})^2}{\left(1 - \frac{x}{d}\right)^2} - \frac{(-V_{ref} - V_{out})^2}{\left(1 + \frac{x}{d}\right)^2} \right] \quad (6)$$

where now d is the gap and x is the accelerometer position. By imposing the nulling of the electrostatic forces we obtain:

$$V_{out} = \frac{x}{d} V_{ref} \quad (7)$$

with a perfectly linear output. To generate such an output the circuit has to calculate the following ratio:

$$\frac{C_1 - C_s}{C_1 + C_s} = \frac{x}{d} \quad (8)$$

A practical implementation of this idea can be seen in the paper by Leuthold et al.[4].

In the third scheme, a feedback electrostatic force keeps the position of the mass close to its equilibrium position. The control signal to keep the seismic mass at rest gives the acceleration. The scheme to implement such idea is shown in figure 8. The moment applied to the seismic mass can be given by:

$$M_{v1} + M_{v2} = F(\alpha) (V_{ref} + V_o)^2 - F(-\alpha) (V_{ref} - V_o)^2 \quad (9)$$

where the function $F(\alpha)$ summarizes the dependence of the moment with the angle. In the case that the control is good enough, we can assume that the mass is at the equilibrium position so $\alpha=0$. Then we have:

$$M_g = M_{v1} + M_{v2} = 4F(0) V_{ref} V_o \quad (10)$$

As M_g is proportional to the sensed acceleration, the output signal is also proportional. The simulation will provide us a less simplified view of the performance of such method.

5. Analysis of the relative performance in static conditions

The implementation in HDL-A of the accelerometer and the functional description of the three interfacing schemes permits a fast evaluation of the performance in static conditions. This exploratory analysis suppresses the necessity of long simulations with circuit level descriptions and permits to choose the more promising interfacing scheme. Next a more detailed analysis of the method of choice can be carried out.

Among all the methods, the charge amplifier gives the more non-linear input-output characteristics. The measured non-linearity is about -38 dB (relative to full scale) in the range between -5 g and 5 g. For our torsional accelerometer charge-balance ceases to be 'perfect' and provides a non-linearity error of -50 dB. Finally, force-balance improves this figure to -60 dB. From this results we decided to carry out a more detailed analysis of the force-balance scheme. The schematic can be shown in figure 9 and it is a modification of the charge-balance proposal by reference[10].

6. Detailed analysis of the force-balance interface

Firstly, we are going to analyze the operation of this switch capacitor interface for both states of the clock signal. In the 0 state all the capacitors C_1 , C_s , C_{off} , C_f , C_b are charged to $V_o[n-1]$. In the 1 state, C_1 is charged to $V_{ref}-V_o[n-1]$, C_s to $-V_{ref}-V_o[n-1]$, C_f to $V_p-V_o[n-1]$, C_i to V_p and C_b to $V[n]$. V is the voltage output of the 1st OTA. A charge-balance analysis shows that the output is given by:

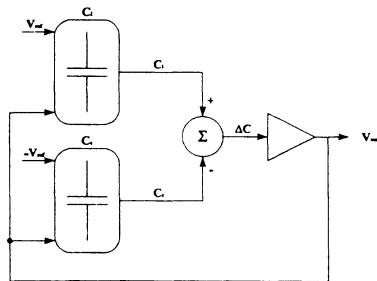


Fig. 8 Functional scheme of a force-balance interface.

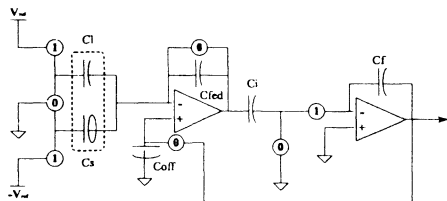


Fig. 9 Schematic of the force-balance interface.

A charge-balance analysis shows that the output is given by:

$$V_o[n] = \frac{C_i}{C_o} \frac{C_l - C_s}{C_r} V_{ref} + V_o[n-1] \quad (11)$$

However, we have to remember that $C_l - C_s$ also depends on the V_o through the electrostatic forces. A more lengthy analysis shows that the net effect of this feedback on the transfer function of the accelerometer is the addition of a real pole.

To simulate the interface circuit we have to decide the level of abstraction we desire for the OTAs. We can choose from a transistor description, a macromodel or a behavioral model. We have chosen the later in order to have a simple description but simultaneously adding some non-idealities as output impedance, frequency response or saturation effects. It includes:

(i) input stage: The effective input signal can be described by three parameters: (a) differential mode, (b) Common mode and (c) Offset voltage. The input impedance is assumed to be infinite.

(ii) Frequency stage: The behaviour of the OTA is described as a second order system

(iii) Gain stage: Includes a voltage controlled current source including saturation effects.

(iv) Output stage: Takes into account the output impedance of the OTA and limits the output voltage.

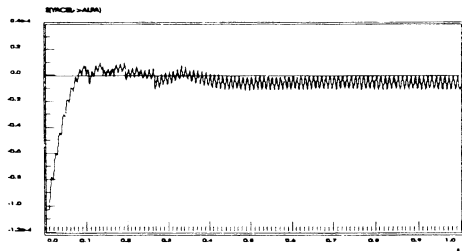


Fig. 10 Transient of the mass position after an acceleration step of 1g.

The static analysis of the force-balance circuit has shown very similar behaviours to the previous functional description. The non-linearity error is better than -60 dB in the -5g- 5g range. From the dynamic point of view, figure 10 shows how the control system is able to correct the seismic mass angle after a step of 1g. It is possible to observe a residual oscillation with the frequency of the clock signal obviously originated from the switch-capacitor

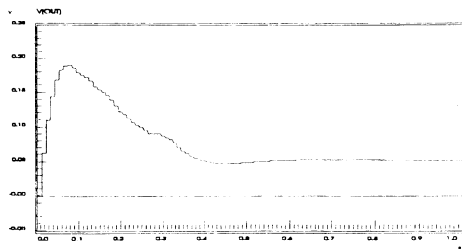


Fig. 11 Transient of the output after an acceleration step of 1g.



nature of the interface. We also observe that the final equilibrium position is not on the 0 angle but slightly lower. This result was not observed in the functional description. Figure X shows the output of the circuit for the same acceleration step.

7. Conclusions

HDL-A has proved to be a useful tool for the analysis of microsystem easing the joint simulation of mechanical system, electronic interfaces and their couplings. In addition, its support of different levels of abstraction allows to carry out analysis at different precision levels easing the top-down design of the microsystem. From our experience simplified functional descriptions of the involved circuits permit to carry out fast exploratory analysis before more detailed analysis are done. This has proved to be specially useful when dealing with switch capacitor interfaces where the time difference between the clock signal and the time-response of the mechanical system can lead to very long computational times.

Acknowledgements

J.M. Gómez-Cama acknowledges a grant from the spanish minister of science and education. This work has been funded by spanish CICYT projects: TIC93-0978-CE and TAP94-1047.

References

- [1] S. Suzuki, S. Tuchitani, K. Sato, S. Ueno, Y. Yokota, M. Sato and M. Esashi, "A Semiconductor Capacitance-type Accelerometer with PWM Electrostatic Servo, Technique," *Sensors and Actuators*, vol. A21-A23, pp. 316-319, 1990.
- [2] O. Ruiz, J. Samitier, S. Marco, J. R. Morante, C. Burrer, and J. Esteve, "Torsional accelerometer with viscous damping control based on thin micromachined silicon structures," presented at TRANSDUCERS'95, Stockholm, 1995.
- [3] D. Herbst and B. Hoeffinger, "Integrated Interface Circuits for Capacitive Micromechanical Sensors," in *Analog Circuit Design*, W. Sansen, Ed. Amsterdam: Kluwer Academic Pub., 1994, pp. 141-162.
- [4] H. Leuthold and F. Rudolf, "An ASIC for High-Resolution Capacitive Microaccelerometers," *Sensors and Actuators A*, vol. 21-23, pp. 278-281, 1990.